J Therm Anal Calorim (2010) 101:89–95
DOI 10.1007/s10973-009-0435-3

Sestak–Berggren function in temperature-programmed reduction

G. Munteanu · E. Segal

Received: 13 July 2009 / Accepted: 18 August 2009 / Published online: 11 September 2009

Abstract From the peculiarities of Temperature-programmed reduction (TPR) method and using the Sestak–Berggren conversion function, we describe first the TPR curve simulation procedure. The influence of the Sestak–Berggren exponents on the TPR peak maximum and shape is demonstrated, by analyzing several synthetic TPR profiles. Finally, the kinetic parameters of Au/CeO_2 promoted with yttrium as well as those of Au/CeO_2–Al_2O_3 promoted with V_2O_5 are discussed.

Keywords Temperature-programmed reduction · Conversion function · Sestak–Berggren exponents · Kinetic parameters

Introduction

Temperature-programmed reduction (TPR) is a powerful technique to study the reduction behavior of the oxidic catalyst precursors [1–3]. It consists of linear heating of the studied sample in a flowing reducible mixture which contains hydrogen. Analyzing the thermogram, i.e., the function *hydrogen consumption* versus *temperature*, one can obtain important information regarding the influence of the structural characteristics such as the nature of the support or promoters on the catalyst reducibility. While doing this, one has also to take into account that the thermogram's shape may also be influenced by some experimental parameters [4, 5]. This influence can be limited, taking into account the recommendations of Monti and Baiker [4], i.e., by correlating the value of the hydrogen concentration in the reducing mixture, its flow rate and sample's mass, and keeping them constant in all the experiments.

When one analyzes the TPR data kinetically, one has to use at least three different thermograms that correspond to different TPR experiments, performed with three different heating rates. As in the case of thermal analysis, one considers that the reaction rate depends on temperature according to Arrhenius law and on physico-geometrical properties of the solid-state phase reactant

$$\beta\frac{\mathrm{d}\alpha}{\mathrm{d}T} = A \cdot \exp\left(-\frac{E}{RT}\right) \cdot f(\alpha) \tag{1}$$

The activation energy is determined using an isoconversional method—similar to that of Friedman [6], i.e., by choosing in those three thermograms points which correspond to the same conversion degree, and plotting $\ln(\beta\frac{\mathrm{d}\alpha}{\mathrm{d}T})$ vs. the reverse temperature, $1/T$. In this way, the activation energy, E, as a function on the degree of conversion, α, is determined.

In the above equation, β is the heating rate, A is the pre-exponential factor, R is the gas constant, and $f(\alpha)$ is the conversion function. This function expresses the concentration of the solid-state phase reactant as a function of the conversion degree taking into account both its physico-geometrical properties and the phenomena which appear during the reduction process.

While proceeding in this manner, one may see whether the activation energy depends or not on the conversion degree. The dependence of the pre-exponential factor on the conversion degree can be determined giving a form to the conversion function. Sometimes, for certain forms of

G. Munteanu (✉)
"Ilie Murgulescu" Institute of Physical Chemistry, 202 Splaiul Independentei st, Bucharest, Romania
e-mail: gmunteanu@icf.ro

E. Segal
Faculty of Chemistry, Physical Chemistry Department, Bucharest University, Bucharest, Romania

the conversion function, one may note a linear dependence of ln$A$ on the activation energy, E, i.e.,

$$\ln A = a \cdot E + b \tag{2}$$

the so-called compensation effect being evidenced [7]. Analyzing the TPR data iso-conversionally, one may evidence distinct stages of the reduction process even when the thermogram suggests a single reduction reaction, i.e., when the thermogram has one single maximum, and no shoulder could be observed [8].

The kinetic triplet, A, E, and $f(\alpha)$, is generally determined either by applying an iso-conversional method, finding first the activation energy, or trying at the beginning to fit the kinetic model and, then, evaluating the activation parameters. We have to mention that in fact the two ways to perform the kinetic analysis are equivalent, in both manners obtaining very close results [9, 10].

There are various forms of the conversion function, with their analytical expressions depending both on the shape of solid-state grains and on the intergranulary, surface or bulk phenomena which have to be described. One such form is that of Sestak and Berggren [11]

$$g(\alpha) = \alpha^m \cdot (1-\alpha)^n \cdot [-\ln(1-\alpha)]^p \tag{3}$$

It was introduced to cover the most thermal analysis (TA) curve shapes. It was believed, for a long time [12], that, indeed, three parameters—m, n, and p—are necessary to describe TA curves, until it was shown [13] that only two parameters are enough.

The corresponding simplified form

$$g(\alpha) = \alpha^m \cdot (1-\alpha)^n \tag{4}$$

is known in literature as Sestak–Berggren SB(m,n) kinetic model, which is used especially in thermal analysis. This kinetic model, together with others, was carefully analyzed [14] showing how to determine the pre-exponential factor, to eliminate false compensation effects, to determine the invariant activation energy, and to determine the true values of Sestak–Berggren exponents, m and n.

As mentioned above, the SB(m,n) kinetic model is also applied in kinetic analysis of the TPR data. As in the case of TA, this kinetic model practically covers the most shapes of the TPR profiles—the values of m and n exponents giving satisfactory explanations to the phenomena being developed during the TPR reaction. For example, while studying the reduction of Fe_3O_4 promoted with copper, we found [8] a value of 0.3 for both m and n. This value is suitable because the system studied contains metallic particles, and the reduction processes take place mainly along the boundary between the oxide and metallic particles [15].

We showed recently [16] that while performing a kinetic analysis of the TPR data, one always has to use for the reaction rate an equation (see next section) that explicitly takes into account its dependence on the experimental parameters. Otherwise, significant errors could affect the results, possibly resulting in a false dependence of the kinetic parameters on the reduction degree.

A very special attention has to be given to the cases in which only the simulation of the TPR profiles can be used to determine the kinetic parameters. In such cases, apart from the influence of the kinetic and experimental parameters on the shape of the TPR profile other factors also have to be taken into account. The values of the m and n Sestak–Berggren exponents have carefully to be chosen, taking also into account their influence on the shape of the TPR profile.

In this article, after a short description of the simulation procedure of the TPR profiles, the main influences of the m, n Sestak–Berggren exponents on the shapes of the TPR profiles will be presented. Knowing this and having taken into account the meaning of their parameters [17], the values of the kinetic parameters will be better determined using TPR curve simulations.

TPR curve simulations

Simulation of any TPR process is based on numerical integration of the reaction rate equation. As far as the TPR process develops one or more reduction reactions, we need to integrate one or more differential equations, using, for example, Runge–Kutta fourth-order method [18].

The simulation of any thermogram begins with assigning of numerical values to the experimental parameters, specific to the TPR experiment in which the thermogram was obtained, which explicitly appear in the reaction rate relationship [5]:

$$\frac{\mathrm{d}c_{\mathrm{ox}}}{\mathrm{d}t} = \frac{2 \cdot D_0 \cdot c_{\mathrm{in}}}{V_r \cdot \frac{p}{p_0} \cdot \frac{T_0}{T} + \frac{2 \cdot D_0}{A \cdot c_{\mathrm{ox}}} \exp\left(\frac{E}{RT}\right)} \tag{5}$$

where D_0 is the flow rate of the reducing mixture in normal conditions, c_{in} is the hydrogen concentration at reactor inlet, V_r is the volume of the reaction space, p and T, respectively, is the pressure and temperature in the reaction space, p_0 and T_0 are the normal values of the same quantities, c_{ox} is the oxide concentration, A is the pre-exponential factor, E is the activation energy, R is the gas constant, and t is the time.

The values of the kinetic parameters are determined by simulation giving them successively various numerical values till one obtains a good fit of the simulated TPR profile with the experimental one.

During the numerical integration process, one takes into account that at a certain moment, when the degree of

reduction is α, the amount of the oxide that directly reacts with the hydrogen is given by

$$c_{ox} = k_{m,n}\frac{m^0_{ox}}{V_r}\cdot \alpha^m(1-\alpha)^n \quad (6)$$

where m^0_{ox} is the initial mass of the oxide that has to be reduced. In this relationship, $k_{m,n}$ is a constant defined by

$$k_{m,n}\cdot\int_0^1 \alpha^m\cdot(1-\alpha)^n d\alpha = 1 \quad (7)$$

Owing to this fact, even if during the simulation process the values of the Sestak–Berggren exponents m and n are changed, the value of the total hydrogen consumption remains unchanged, the TPR profile area remaining the same. We have to mention that in any situation when $m \neq 0$, we consider, at the beginning, and during the induction period, that $\alpha = 0.001$ till the moment, when due to the reduction process, the reduction degree becomes higher then this value. In other words, only after having a reduction degree higher than 0.001, one may state that metal particles exist on the surface and the reduction process takes place around them; till then, the reduction mechanism is different. Only after having a reduction degree higher than this value, one may use SB(m,n) conversion function.

In order to determine the effects of the Sestak–Berggren exponents on the shape of the TPR profile, we simulated a series of TPR curves using in all the calculations the same values for the activation parameters: $A = 6 \times 10^8$ m^3/mol s and $E = 76$ kJ/mol. The values of the experimental parameters were those obtained from real TPR experiments: the flow rate is $D_0 = 25$ mol/min, the heating rate is $\beta = 15$ deg/min, hydrogen concentration in the reducing mixture is $c_{in} = 10\%$ (4.46 mol/m^3), the pressure in reactor being that of normal, i.e., 101325 Pa and reaction volume 0.2 cm^3. We considered that the total amount of the oxide that has to be reduced is 58 μmol (MO type, were M is a divalent metal); consequently, its concentration is 290 mol/m^3.

Results and discussion

In our simulation, we systematically varied the values of the Sestak–Berggren exponents, m and n, using the above experimental parameters. Apparently, the cases, when $m = 0$, i.e., in cases of the so-called self-constricting sphere model, are completely different of the others. Only in these cases, when $m = 0$, the function $g(\alpha)$ monotonically decreases from 1 down to zero: the higher the value of n, the higher the slope of this decrease. In all the other cases, when both $m \neq 0$ and $n \neq 0$, this function reaches a maximum for a value of α that depends on both m and n:

$$\alpha_{max} = \frac{m}{m+n} \quad (8)$$

As mentioned above, the cases, when $m = 0$ and $m = 0.1$, would have to be very different. This would be because in the first case, when $m = 0$ we have $g(0) = 1$, whereas in the other case g(0) = 0 when $m = 0.1$.

In Fig. 1a, b, we plotted the values of $k_{m,n}\cdot g(\alpha)$ both for $m = 0$ and $m = 0.1$, respectively, with the exponent n having various values. The normalizing parameter, $k_{m,n}$, takes different values which depend on m and n, to satisfy Eq. 7. In this figure, we may see that, indeed, $g(0) = 1$ when $m = 0.0$, and $g(0) = 0$ when $m = 0.1$, but excepting in a very narrow vicinity of $\alpha = 0$, for any value of n, the corresponding curves are quite similar. The natural consequence of this fact is that in both cases one obtains very similar TPR profiles. Significant differences are obtained only when we have very large pre-exponential factors, i.e., when we have very narrow peaks.

As we may see in Fig. 2, the two TPR profiles, simulated with $m = 0.0$ and $m = 0.1$, but the same Sestak–Berggren exponent $n = 0.7$, are very similar. In simulations, when

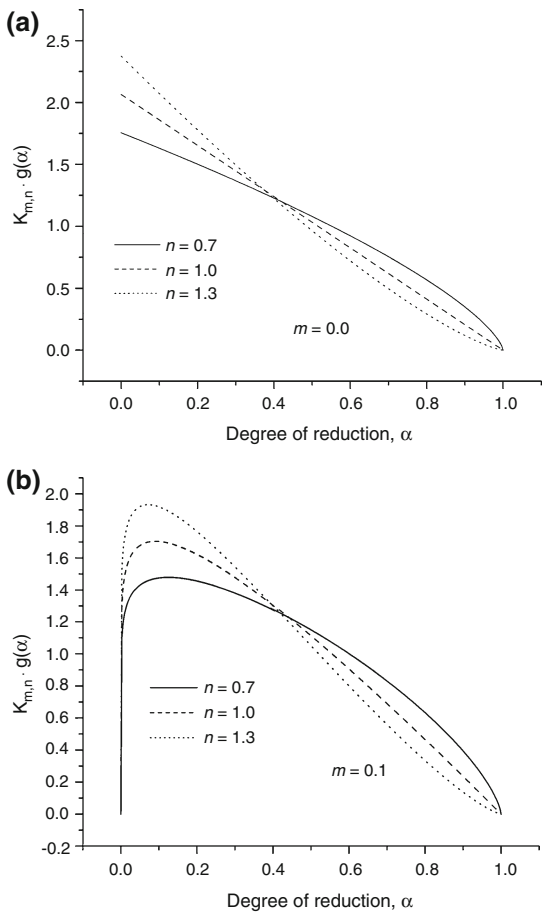

Fig. 1 The Sestak–Berggren function for several usual values of n exponent: 0.7, 1.0, and 1.3. **a** $m = 0.0$, **b** $m = 0.1$

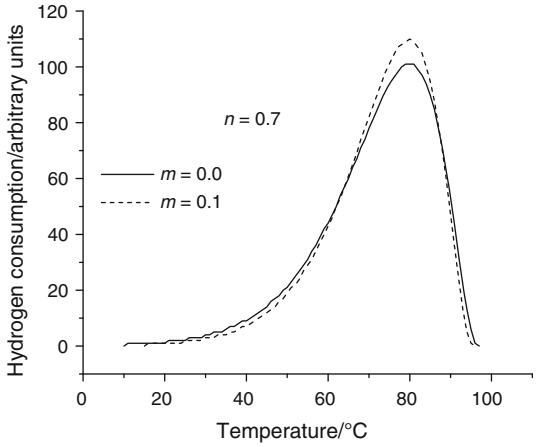

Fig. 2 The TPR profiles simulated with the same value for $n = 0.7$ and two different values for m: 0.0 and 0.1

one has to generate a simulated thermogram that consists of at least two overlapping peaks, such differences are not significant.

Coming back to relationship (8), we note that for a given m, the higher the n, the lower the value of α_{max}, but for a given n, the higher the m, the higher the α_{max}, too. These facts have, as we shall see, influence on the symmetry of the TPR profiles. In order to understand this, we have to take into account that having α_{max} higher and higher means having the most part of the oxide reduced at higher and higher temperatures. This means that by changing the Sestak–Berggren exponents in such a way that α_{max} increases, one shall obtain an increase in the maximum temperature of the TPR peak. On the other hand, increasing the amount of the oxide that is reduced at higher temperatures where, according to Arrhenius law, the reaction rate is higher, means decreasing the time in which it is reduced. In other words, the TPR peak will become narrower and asymmetric, the half-width of the high temperature region becoming smaller. This is exemplified in Fig. 3.

Taking into account the facts presented above, we can now complete those that we wrote above in respect of relationship (8). As we stated before, for a given m, the higher the n, the lower the α_{max}; this means, as we can see in Fig. 4a, that on increasing the value of n, the TPR profile will become enlarged, becoming more symmetric, and its maximum being shifted towards low temperature region. Figure 4b shows that by keeping the value of n constant and increasing the values of m, the TPR profiles become more and more narrow, the temperature of their maxima becoming higher and higher; as we showed before; this happens because α_{max} becomes higher and higher.

All the above statements have to be taken into account when, to determine the kinetic parameters, a TPR profile is simulated. Because even when the TPR profile consists of only one peak, it is possible to generate various simulated

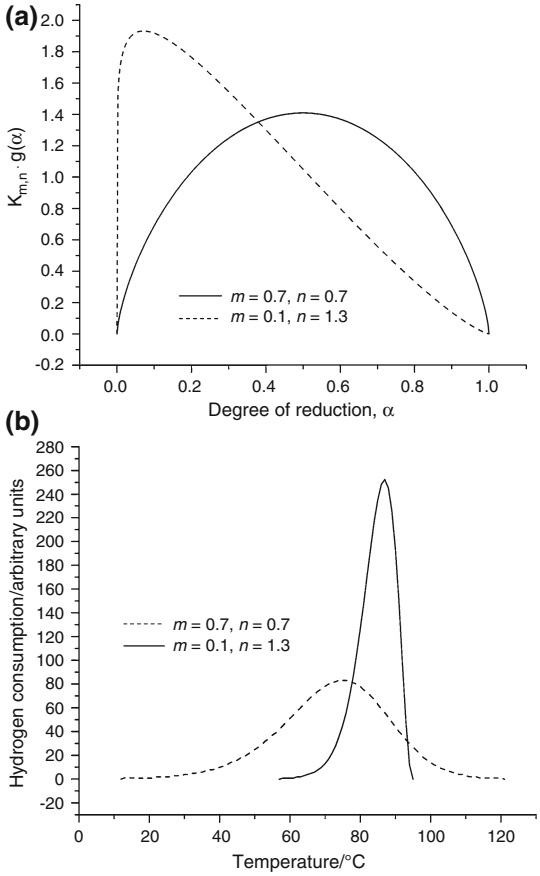

Fig. 3 The effect of the change of the Sestak–Berggren exponents. **a** the conversion function; **b** the TPR profiles

curves that fit the experimental TPR curve very well; in the simulation process, however, it is not enough to take into account only the fit criterion. It is necessary to take into account the meaning of the Sestak–Berggren exponents [17] in correlation both with the structure of the sample as well as the reduction mechanism.

In the following, we shall give several examples. Two of them—Fig. 5a—represent the cases of the reduction of fresh gold catalyst supported on ceria doped with yttrium and of the same catalyst after re-oxidation at 100 °C. As one may see, each consists of one isolated peak. The third case i.e., the reduction of gold supported on ceria–alumina mixture promoted with vanadia, is more complex. It apparently consists, if we take into account the number of peaks in the thermogram, of at least two different reduction process.

In Fig. 5a, one may see that the two thermograms due to Au/CeO_2 catalysts doped with yttrium, the fresh one and that re-oxidized, have very different shapes, their maxima being located at different temperatures. The values of the Sestak–Berggren exponents, of the activation parameters and λ coefficient—see Eq. 9, which may be seen in Table 1, were chosen according to those described above as well as the meaning of the Sestak–Berggren exponents [17].

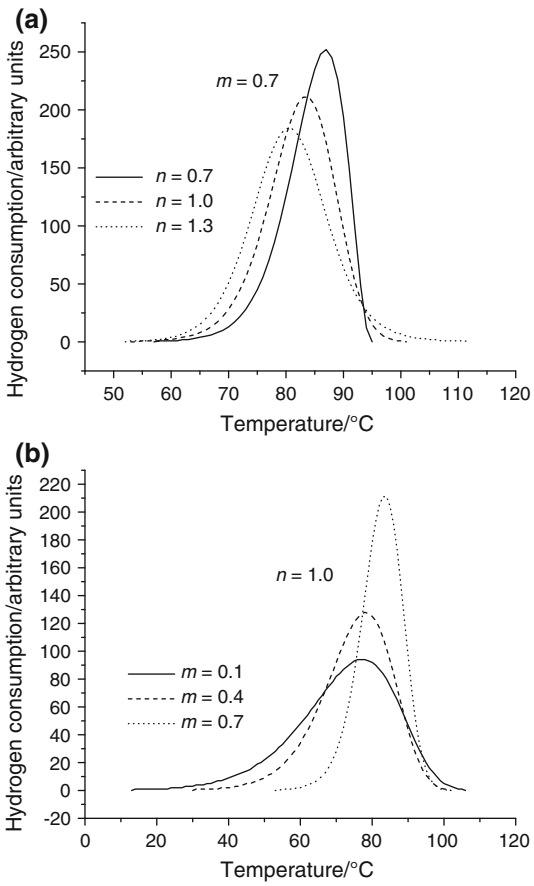

Fig. 4 **a** On increasing the value of n and keeping the value of m constant, the TPR profiles become larger and larger, with the temperature of their maxima decreasing. **b** When the value of m increases, with the value of n remaining constant, the TPR profiles become more and more narrow, with the temperature of their maxima increasing

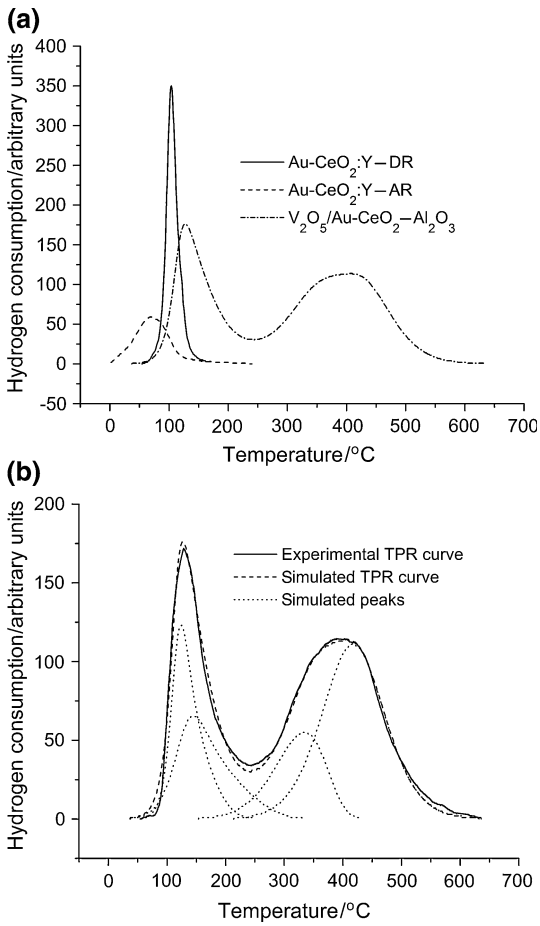

Fig. 5 **a** The TPR profiles of Au/CeO_2:Y fresh and re-oxidized in air at 100 °C after reduction as well as the TPR profile of 4% V_2O_5–Au/CeO_2–Al_2O_3 catalyst. **b** The experimental and simulated TPR profile of 4% V_2O_5–Au/CeO_2–Al_2O_3 catalyst together with the simulated individual peaks

In Table 1, we note that the values of the activation energy for these two TPR processes are very different. This difference has an insignificant influence on the values of the reaction rate. In the temperature ranges in which the corresponding peaks appear, around 100 °C, the two exponentials have both values very close to one.

The above observation reveals that in this case, of the two Au/CeO_2 catalyst samples doped with yttrium, the main effect on the reaction rate is due to the pre-exponential factor. As one may see in Table 1, the value of fresh sample is with six magnitude orders higher than that of the re-oxidized sample. This is mainly due to the fact that in case of the fresh sample, the TPR profile is very narrow compared to that of the other sample. This very important difference could allow us to state that only in case of the fresh sample, gold manifests its catalytic effect. In this case, around gold particles, various oxygen species are concentrated, and during the TPR of this sample, these oxygen species are removed. This fact is proved by the value of the exponent m: its value is 0.5, and this means that the reduction takes place around gold particles.

One may state that during this reduction, the oxygen species are also removed from the structure of CeO_2 located in the very close vicinity of gold particles. This is proved by the value of the parameter, λ. As we showed before [17] in our simulations, we considered that the activation energy could depend on the degree of reduction according to the equation

$$E = E_0(1 + \lambda \cdot \alpha) \tag{9}$$

The non-zero value of λ, though very small, proves that oxygen atoms, which are a little far from gold particles, are removed, but in a very narrow vicinity.

In the first TPR experiment, that of the fresh sample, the temperature increase up to 200 °C. We must take into account that while removing oxygen atoms from the structure of CeO_2, oxygen vacancies are created in the vicinity of gold particles. Because, at 200 °C, the oxygen

Table 1 The kinetic parameters of fresh and re-oxidized Au/CeO_2 doped with yttrium catalyst sample and of V_2O_5–Au/CeO_2–Al_2O_3 sample

Sample	T_{max} /°C	Proportion/%	A /m^3/mol/s	E /kJ/mol	Sestak–Berggren exponents		λ
					m	n	
AuCeY_CP_DR	104	100	$6.0 \times 10^{+9}$	84.5	0.5	1.3	0.03
AuCeY_CP_AR	96	100	$6.0 \times 10^{+3}$	44.7	0.0	0.8	0.0
V–$Au/CeO_2Al_2O_3$	124	20	$4.8 \times 10^{+6}$	68.1	0.38	1.3	0.12
	143	19.5	$1.2 \times 10^{+5}$	61.8	0.01	0.9	0.18
	331	17	$3.0 \times 10^{+3}$	70.2	0.01	1.3	0.0
	414	43.5	$1.2 \times 10^{+3}$	74.0	0.2	1.3	0.0

has a high mobility in a very short time, after reduction, the oxygen vacancies will be occupied by oxygen atoms from the structure of CeO_2. In other words, the oxygen vacancies will be spread into the structure of the CeO_2 grains. This happens mainly because the yttrium cations, which induce oxygen vacancies, are uniformly distributed in the structure of CeO_2.

At 100 °C, when the reduced sample is re-oxidized, the oxygen vacancies are uniformly distributed in the grains of CeO_2; they are not located any more only in the vicinity of gold particles. Consequently, at 100 °C the sample is uniformly re-oxidized.

The TPR profile of the re-oxidized sample is a consequence of the facts stated above. We have, in this case, a superficial reduction of the sample. We have removed oxygen atoms which are uniformly distributed on the grain's surface.

There are several consequences: (a) the reduction does not take place only around gold particles; it takes place on all the surface of the CeO_2 grains. Owing to this fact m has to be zero, and λ also has to be zero. In Table 1, we may note that indeed it is so, but we also note that the value of n decreased from 1.3 to 0.8. This means [17] that in this case the reduction takes place mainly due to an Eley–Rideal mechanism, not due to a Langmuir–Hinshelwood one. This also means that the oxygen atoms, uniformly distributed on the grain surface, after re-oxidizing, are very reactive. This explains both the fact that n is very low and that its reduction starts at significantly lower temperatures. Probably, this is due to the fact that these oxygen atoms are very weakly bonded to the structure of CeO_2 grains.

In case of the sample that consists of Au on CeO_2–Al_2O_3 mixture covered with a monolayer of V_2O_5, the TPR spectrum is more complex. As one may see in Table 1, there are four distinct reduction processes which overlap giving an envelop that apparently has only two maxima.

As one may see in the same table, the four reduction processes have significant weights. The first, with maximum located at 124 °C, is due to the superficial reduction of CeO_2 in the vicinity of gold particles. Owing to this fact, $m = 0.38$ and $\lambda = 0.12$. Since the value of λ is large, we believe that the vicinity of gold particle in which the reduction takes place is large enough.

The second peak with the maximum located at 143 °C is due to the reduction of vanadia species located close to gold particles. Most probably, it consists of an island of CeO_2 around a gold particle followed by a region of vanadia. This is why, in our opinion, the exponent m is almost zero, but λ significantly large.

The other two peaks are due to the partial bulk reduction of the islands of CeO_2 as well as of CeO_2 located in the vicinity of Al_2O_3. We state this because the Sestak–Berggren exponent m is large enough, 0.2. This means that the reduction process develops in the vicinity of a contact boundary between the material which is reduced and the grain that induces the reduction. In our opinion, the grains of Al_2O_3 generate Ce^{3+} around their contact boundary with CeO_2, and these cations initiate the reduction of CeO_2.

According to the values of n, Sestak–Berggren exponent [17], the only reduction that takes place due to an Eley–Rideal mechanism is in the case of vanadia, while all the others are developed due to a Langmuir–Hinshelwood one.

Conclusions

Taking into account the above presented facts, we may state that the Sestak–Berggren conversion function is a helpful tool in the kinetic analysis of the TPR data. It significantly helps both in simulations, to fit well the simulated curves with the experimental ones, as well in choosing the adequate values of the kinetic parameters according to the sample's structure.

References

1. Falconer JL, Schwarz JA. Temperature-programmed desorption and reaction: applications to supported catalysts. Catal Rev-Sci Eng. 1983;25:141–227.
2. Bhatia S, Beltramini J, Do DD. Temperature programmed analysis and its applications in catalytic systems. Catal Today. 1990;7:309–438.

3. Hurst NW, Gentry SJ, Jones A, McNicol BD. Temperature programmed reduction. Catal Rev-Sci Eng. 1982;24:233–309.
4. Monti DAM, Baiker A. Temperature programmed reduction. Parametric sensitivity and estimation of kinetic parameters. J Catal. 1983;83:323–35.
5. Munteanu G, Craiu M. Influence of the experimental parameters on the TPR profiles. React Kinet Catal Lett. 1993;50:49–54.
6. Friedman HL. Kinetics of thermal degradation of char-forming plastics from thermogravimetry. Application to phenolic plastic. J Polym Sci. 1964;6C:183–95.
7. Andreini A, Poels EK, Bliek A. Evidence for a compensation effect during the temperature programmed-reduction of copper oxide in hydrogen. React Kinet Catal Lett. 1998;63:209–17.
8. Munteanu G, Budrugeac P, Ilieva L, Tabakova T, Andreeva D, Segal E. Kinetics of temperature programmed reduction of Fe_3O_4 promoted with copper: application of iso-conversional methods. J Mater Sci. 2003;38:1995–2000.
9. Pratap A, Rao TLS, Lad NK, Dhurandhar HD. Isoconversional vs. Model fitting methods. J Therm Anal Calorim. 2007;89:399–405.
10. Burnham AK, Dinh LN. A comparison of isoconversional and model-fitting approaches to kinetic parameters estimation and application predictions. J Therm Anal Calorim. 2007;89:479–90.
11. Sestak J, Berggren G. Study of the kinetics of the mechanism of solid-state reactions at increasing temperatures. Thermochim Acta. 1971;3:1–12.
12. Sestak J. Philosophy of non-isothermal kinetics. J Therm Anal Calorim. 1979;16:503–20.
13. Gorbatchev M. Some aspects of Sestak's generalized kinetic equation in thermal analysis. J Therm Anal Calorim. 1980;18:193–7.
14. Koga N, Matek J, Sestak J, Tanaka H. Data treatment in non-isothermal kinetics and diagnostic limits of phenomenological models. Netsu Sokutei. 1993;20:210–23.
15. Sestak J, Satava V, Wendlandt WW. The study of heterogeneous processes by thermal analysis. Thermochim Acta. 1973;7:333.
16. Munteanu G, Miclea C, Segal E. Errors in evaluation of the kinetic parameters in temperature programmed reduction. J Therm Anal Calorim. 2008;94:317–21.
17. Munteanu G, Ilieva L, Nedyalkova R, Andreeva D. Influence of gold on the reduction behaviour of Au–V2O5/CeO2 catalytic systems: TPR and kinetic parameters. Appl Catal A. 2004;227:31–40.
18. Bakhvalov N. Numerical methods. 2nd ed. Moscow: Mir; 1973.